General Camera Calibration Models

Orrin Thomas, Oak Ridge National Laboratory

Michael Manginelli, Nasa, Marshal Space Flight Center

Overview

- The mission, measure Rocket Plume Erosion (RPE)
- Stereo Cameras for Lunar Plume-Surface Studies (SCALPSS)
- Camera calibration data, methods, and models
- The SCALPSS camera calibration data
- Camera model history and categories

Rocket plume erosion

“interaction between the rocket plume and the surface material beneath the vehicle plays a significant role in the descent dynamics and safety[1]”

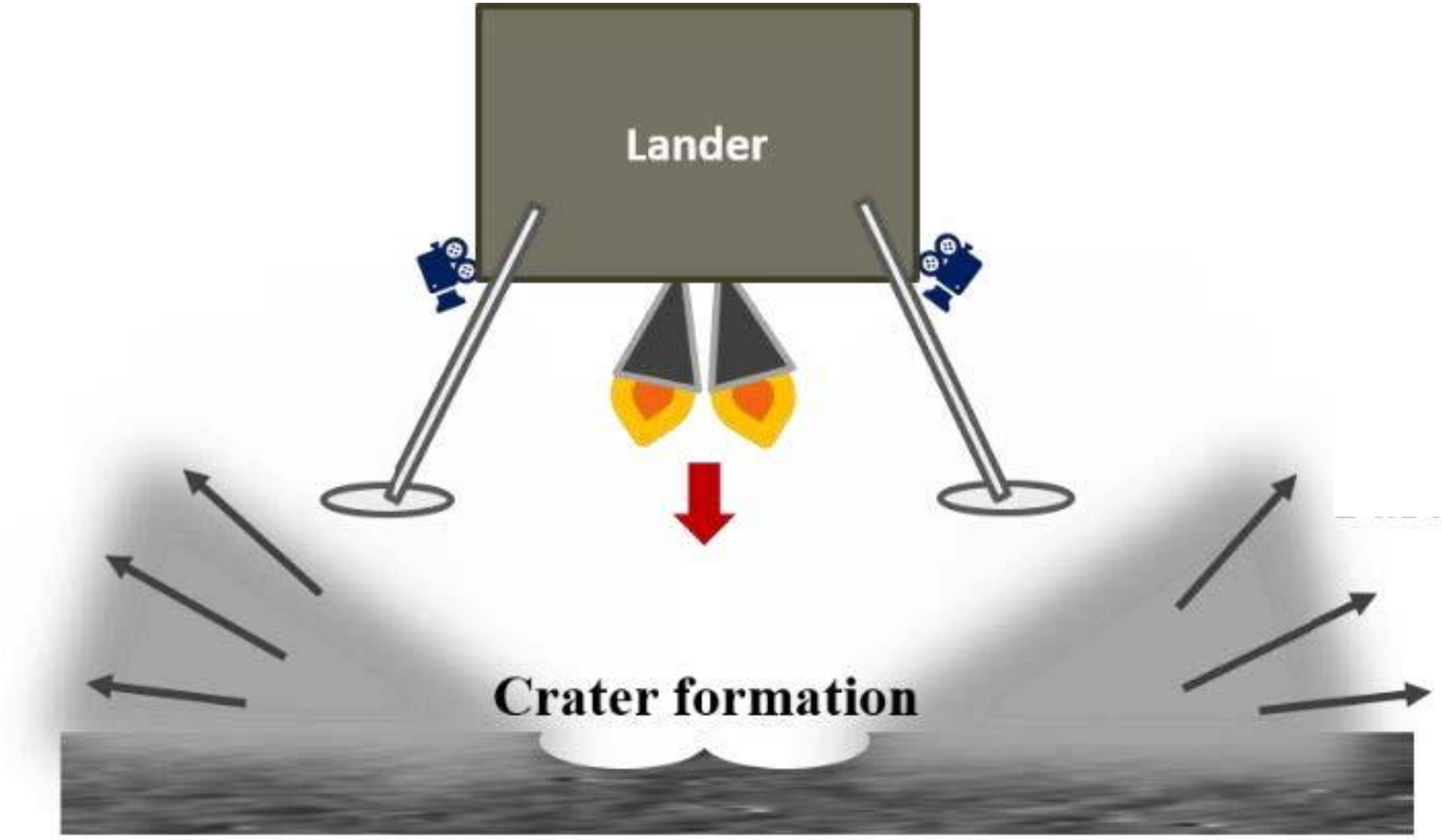

Image Source: [2]

Rocket plume erosion

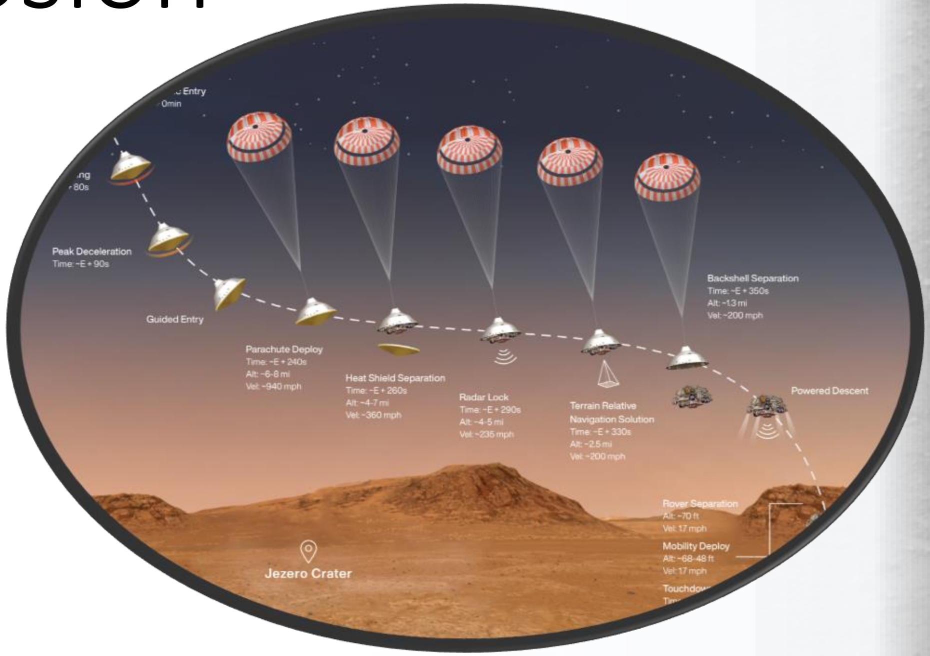

Curiosity Rover

Image Sources:
https://mars.nasa.gov/msl/multime
resources insight-on-mars-illustratio
See: Seven Minutes of Terror

Rocket plume erosion

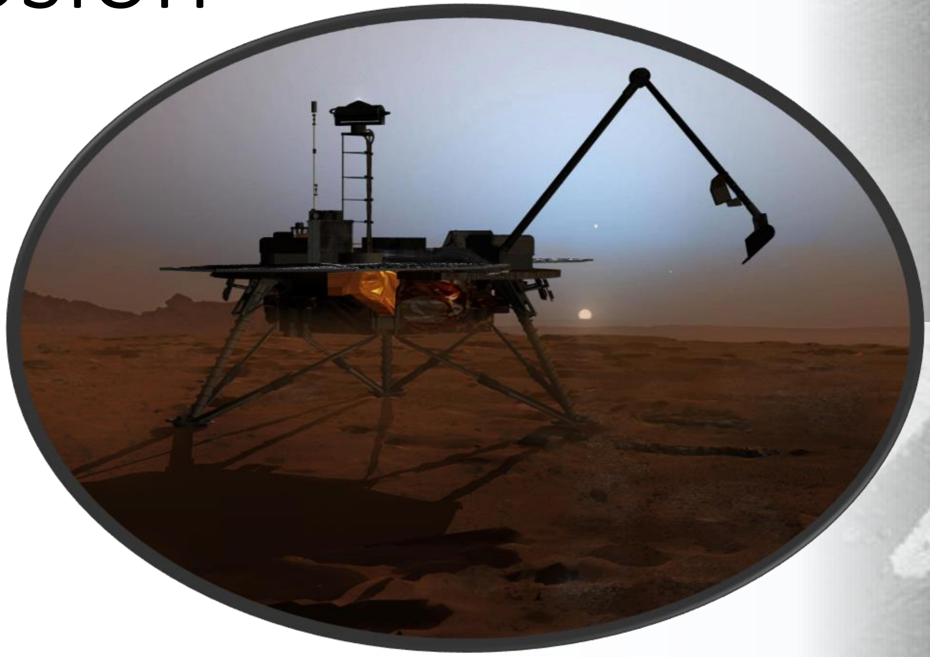

Phoenix Lander

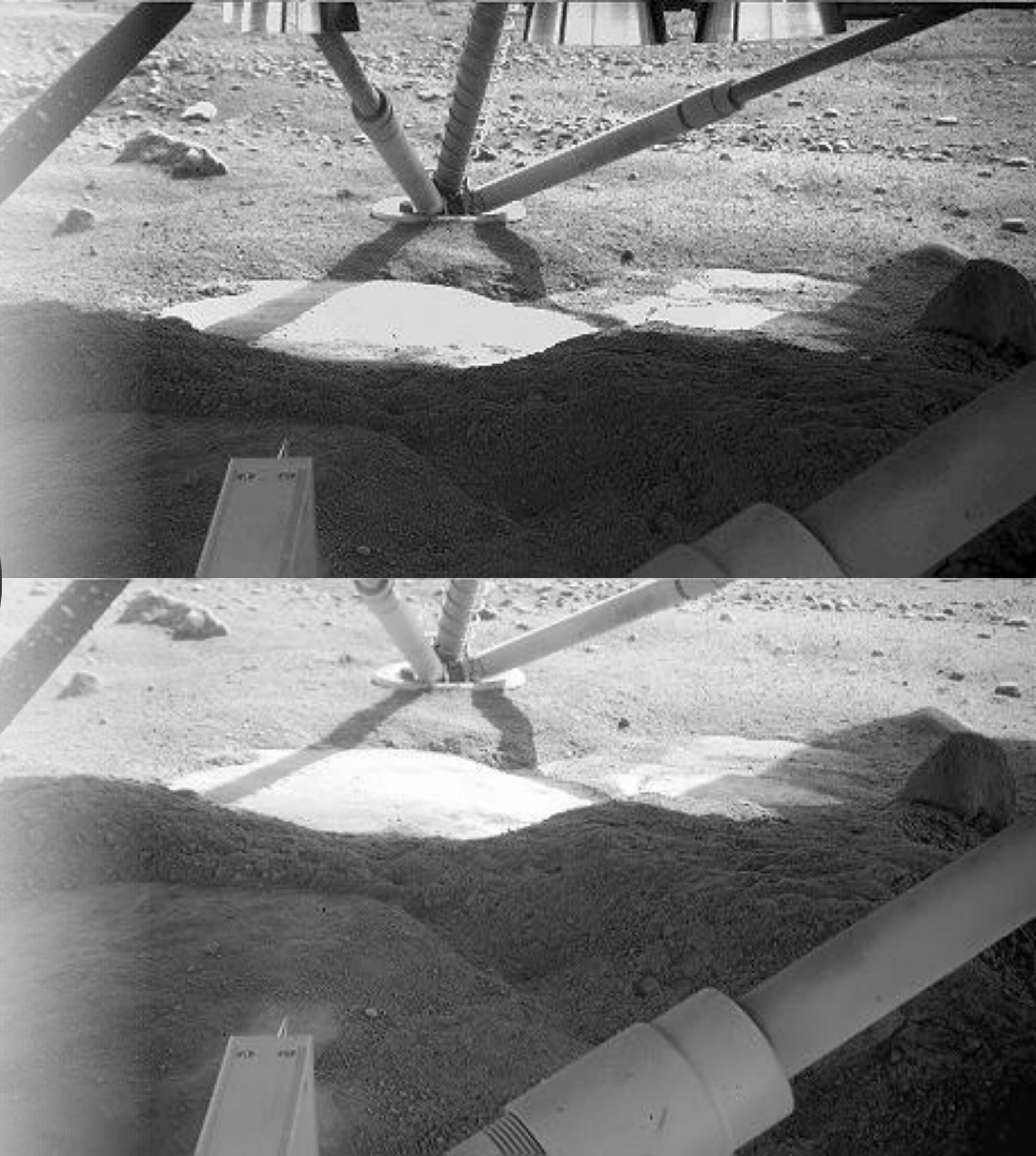

Image Sources:
Jet Propulsion Laboratory PHOTOJOURNAL
NASA Mission pages, Phoenix

Rocket plume erosion

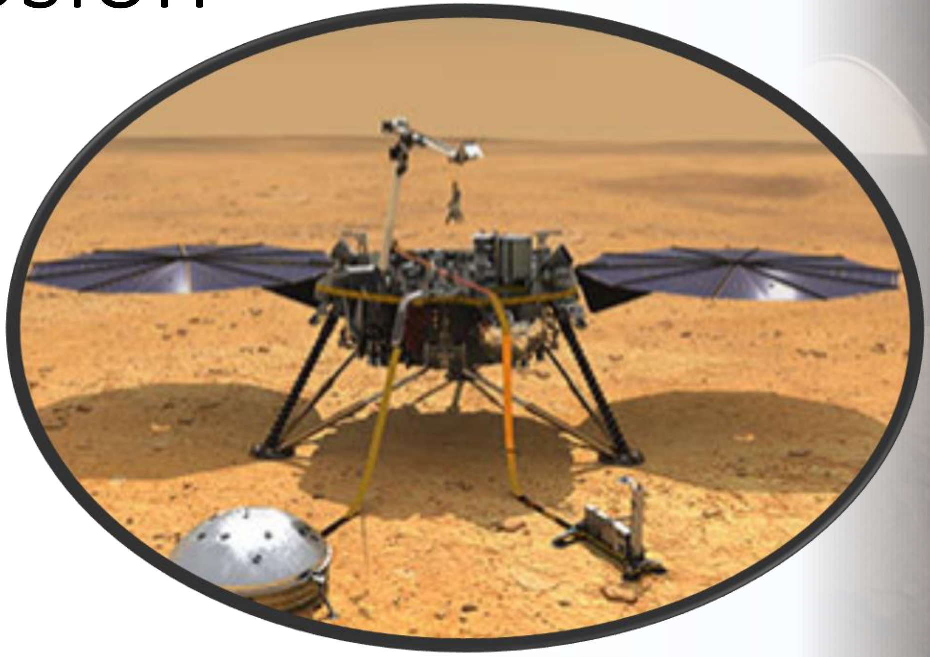

Insight Lander

Image Sources:
https://mars.nasa.gov/insight/
https://mars.nasa.gov/mars-exploration/
missions/insight/

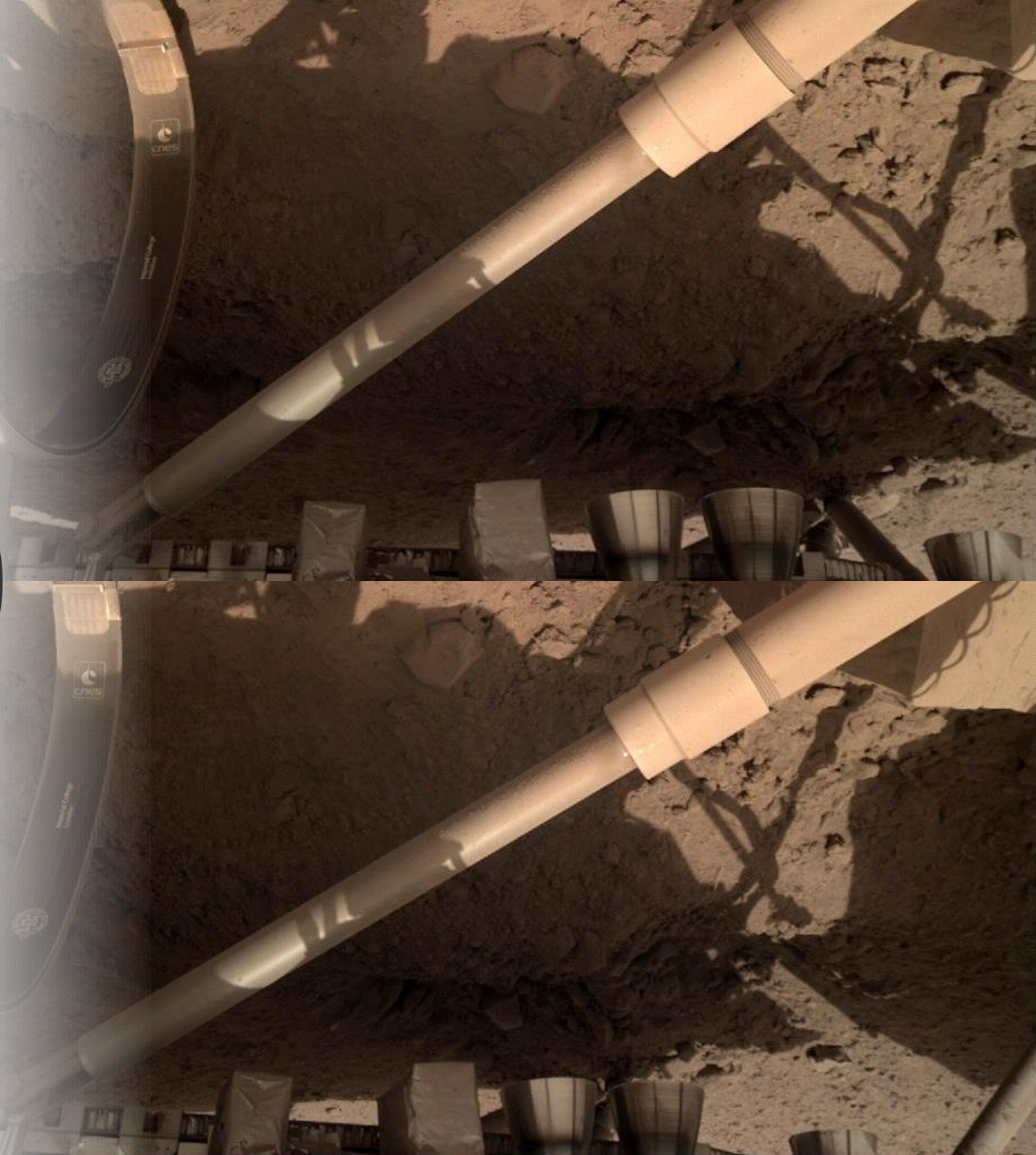

SCALPSS

First Dedicated RPE Study

- Involved in the planning
- Measurements before, during, and after landing.
- Pick cameras and **calibrate** them.

Image Sources: [2]
References: [1-2]

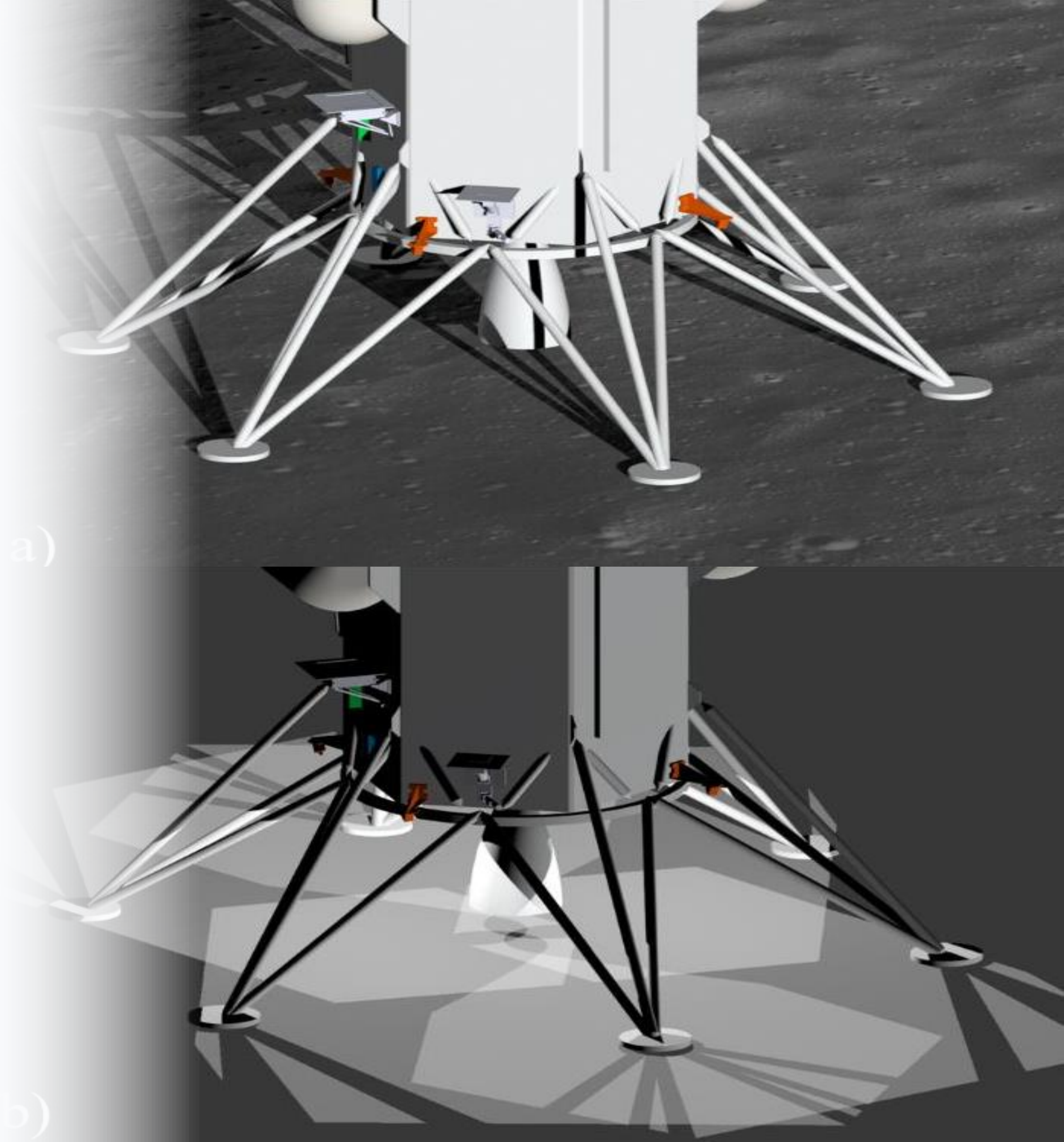

Bouguet Calibration

NASA's Legacy SOP

- Measurements of planar target with targets
- Math model is essentially Brown's model
- Failed!

References: [3-5]

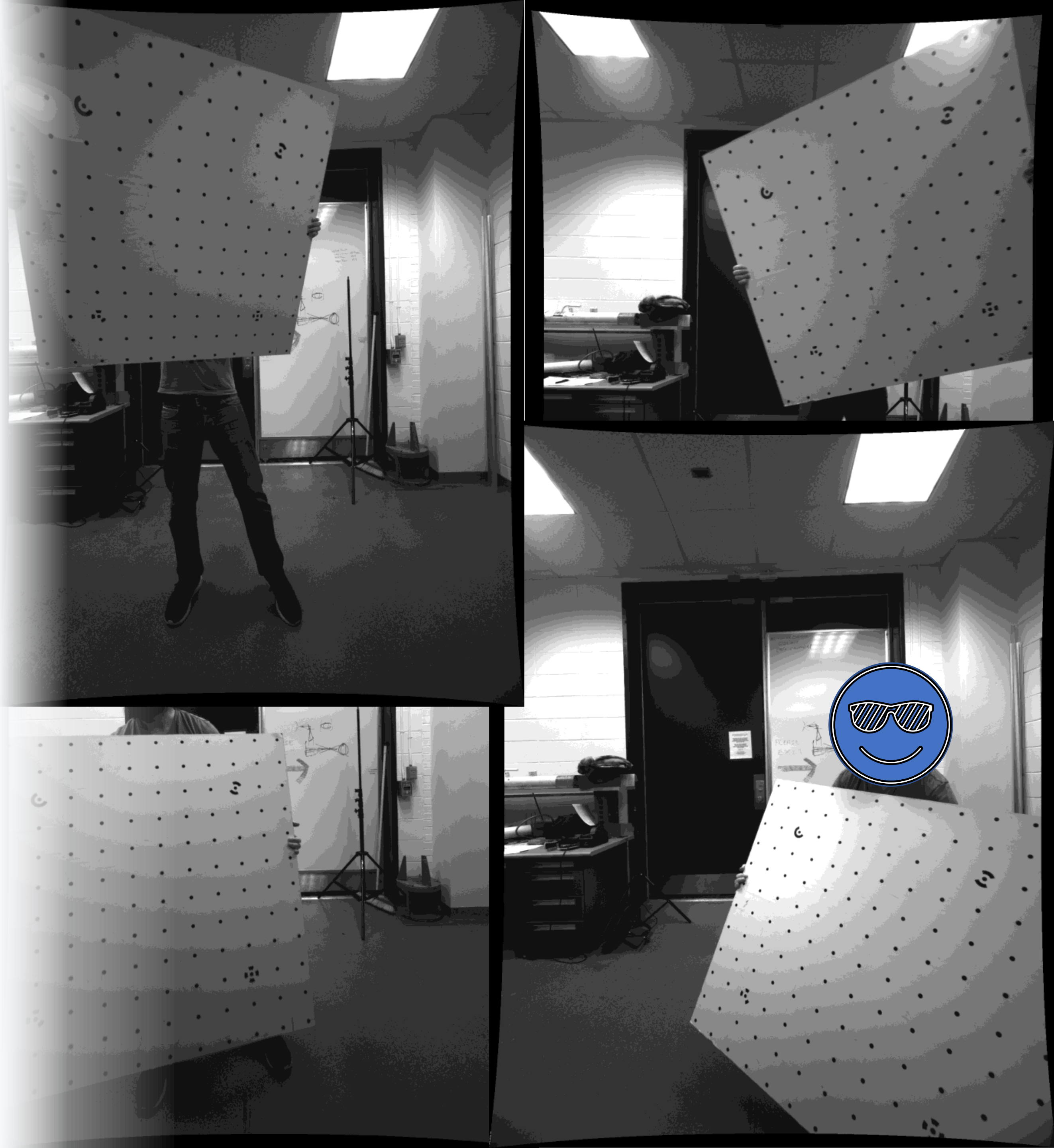

Plan B

- Calibration harp [6-7]
- Rational distortion model [8]
- Two stage calibration for ultimate de-correlation of parameters [9]
- Let the Johnson Space Flight center team do an exterior calibration.

Categorizing Calibration Models

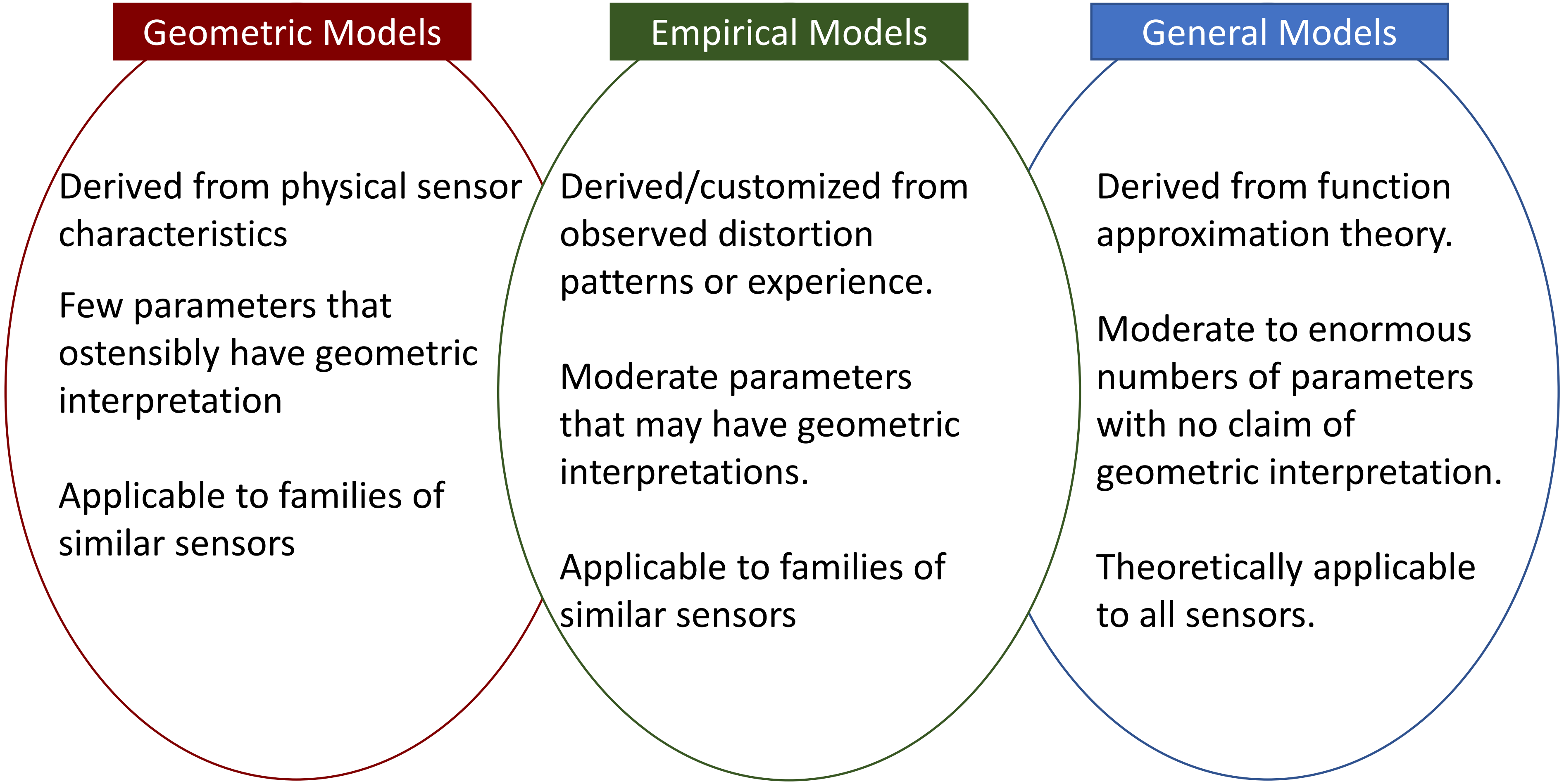

Geometric Models

Derived from physical sensor characteristics

Few parameters that ostensibly have geometric interpretation

Applicable to families of similar sensors

Empirical Models

Derived/customized from observed distortion patterns or experience.

Moderate parameters that may have geometric interpretations.

Applicable to families of similar sensors

General Models

Derived from function approximation theory.

Moderate to enormous numbers of parameters with no claim of geometric interpretation.

Theoretically applicable to all sensors.

Extracted Harp Lines

- 500,000 measurements
- Covering 99.8% of the field of view
- Precision of 0.04 pixels RMSE, consistent with [6,10-11]

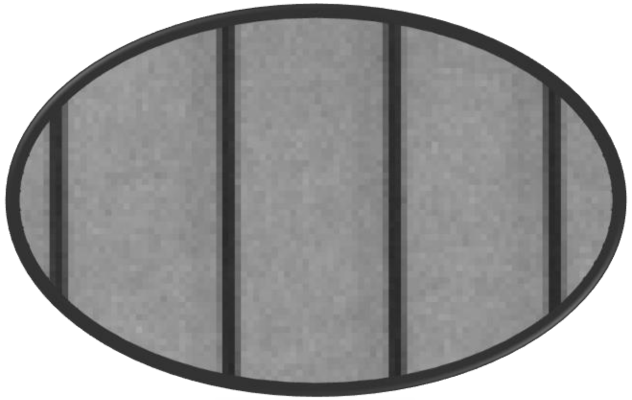

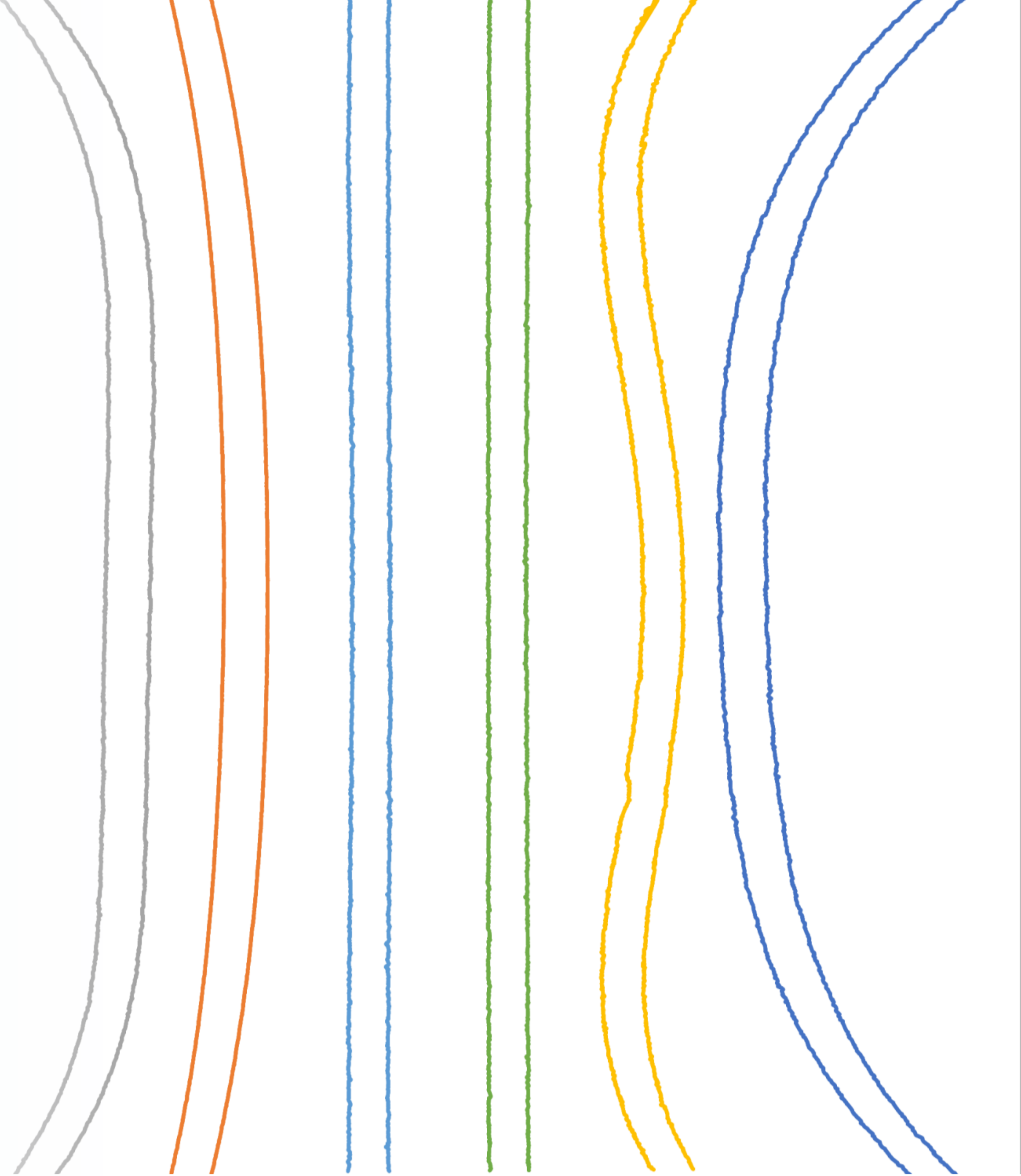

Numerical Solution Path

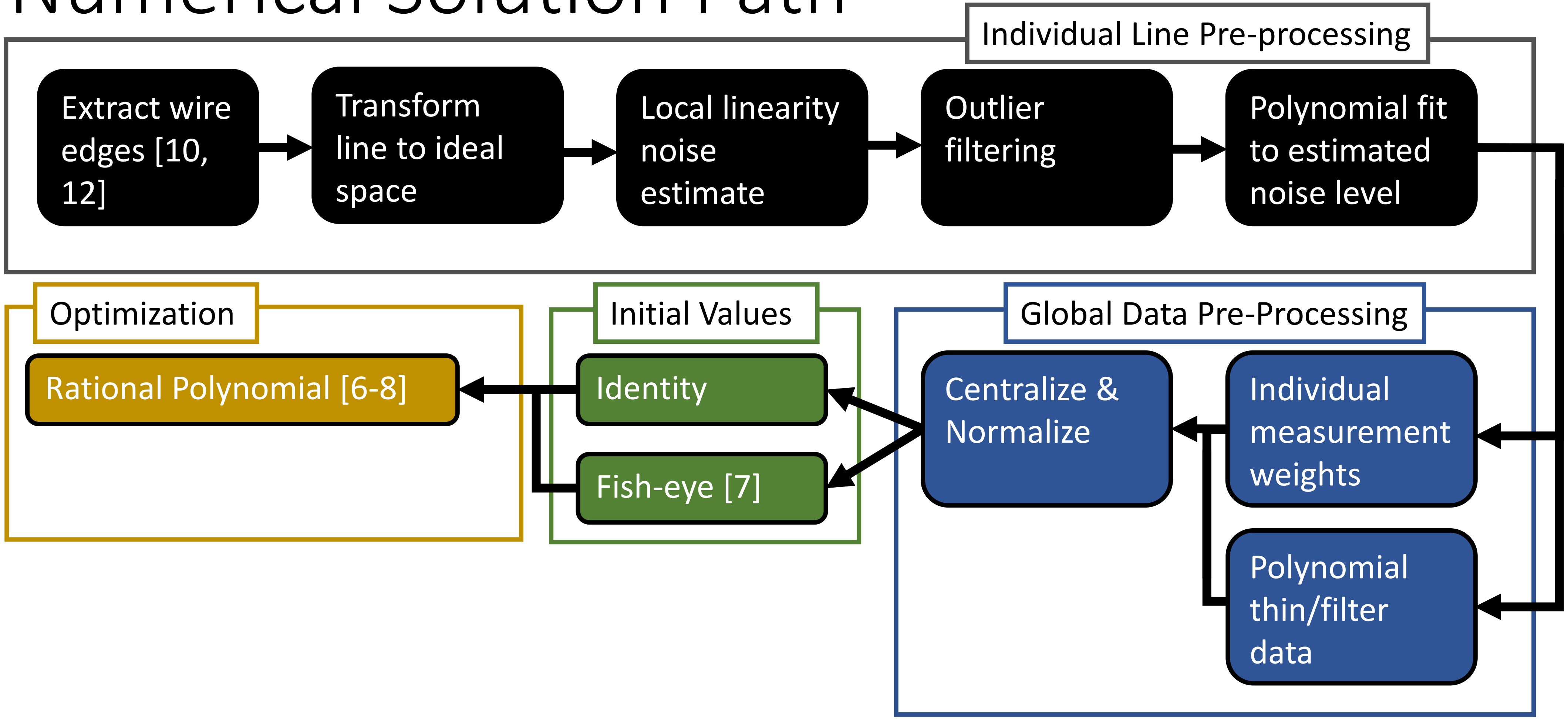

Individual Line Pre-processing

Extract wire edges [10, 12]

Transform line to ideal space

Local linearity noise estimate

Outlier filtering

Polynomial fit to estimated noise level

Optimization

Rational Polynomial [6-8]

Initial Values

Identity

Fish-eye [7]

Global Data Pre-Processing

Centralize & Normalize

Individual measurement weights

Polynomial thin/filter data

Numerical Solution Path

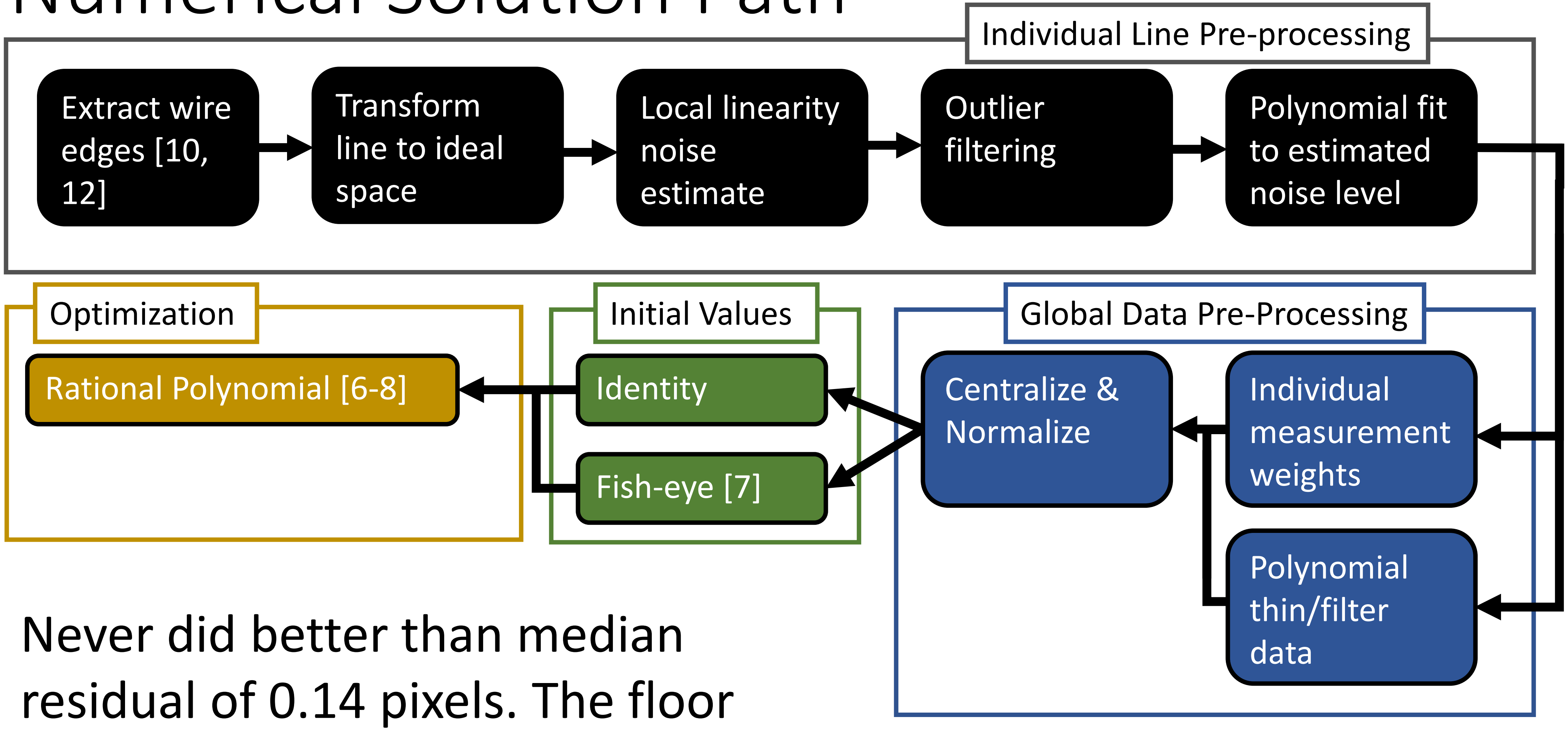

Never did better than median residual of 0.14 pixels. The floor for that value was 0.03 pixels.

Back to literature review

Machine Vision

Research addressing the need to model fish-eye lenses, drone/surveillance cameras

Photogrammetry

Research addressing the need to reduce correlations among parameters in Insitu calibrations.

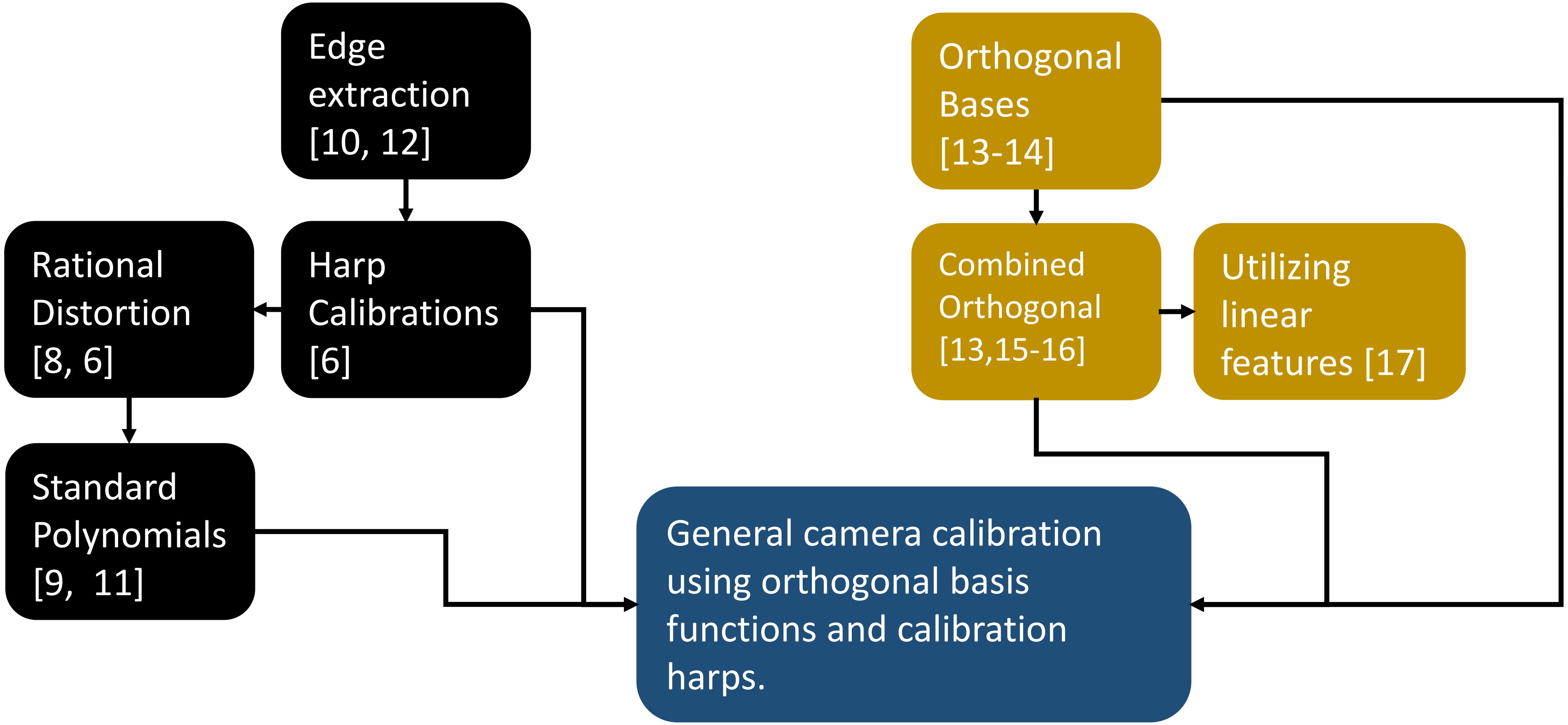

Edge extraction [10, 12]

Harp Calibrations [6]

Rational Distortion [8, 6]

Standard Polynomials [9, 11]

Orthogonal Bases [13-14]

Combined Orthogonal [13,15-16]

Utilizing linear features [17]

General camera calibration using orthogonal basis functions and calibration harps.

Orthogonal Basis Functions

Can theoretically model any arbitrary function, to any arbitrary accuracy (see the Stone-Weierstrass or Fourier Theorem).

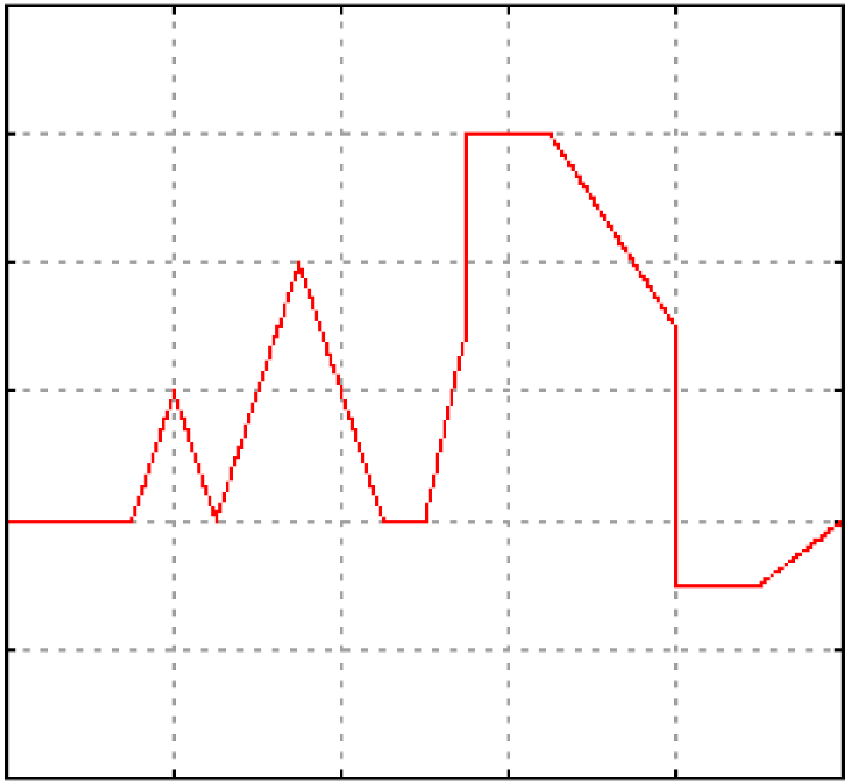

Image Source: Wikipedia commons

2D Orthogonal Basis Functions

$f_{m,n}(x,y) = g_m(x)h_n(y)$ $\int_{-1}^{1}\int_{-1}^{1} f_{m_1,n_1}(x,y)f_{m_2,n_2}(x,y)\, d_x d_y \; = 1,$ if $m_1 = m_2$ and $n_1 = \; n_2,$ else 0

Legendre	Chebyshev (Type 1)	Fourier
1	1	1
x	x	$\sin(\pi x)$
y	y	$\sin(\pi y)$
$(3x^2 - 1)/2$	$2x^2 - 1$	$cos(\pm\pi x)$
xy	xy	$cos(\pm\pi y)$
$(3y^2 - 1)/2$	$2y^2 - 1$	$\sin(2\pi \mathrm{x})$
$(5x^3 - 3x)/2$	$4x^3 - 3x$	$\cos(\pm 2\pi x)$
$(3x^2 - 1)y/2$	$(2x^2 - 1)y$	$\sin(\pi \mathrm{x})\cos(\pm\pi y)$
$(3y^2 - 1)x/2$	$(2y^2 - 1)x$	$\cos(\pm\pi \mathrm{x})\sin(\pi y)$
$(5y^3 - 3y)/2$	$4y^3 - 3y$	$\sin(2\pi \mathrm{x})$
$\vdots$	$\vdots$	$\vdots$

Numerical Solution Path

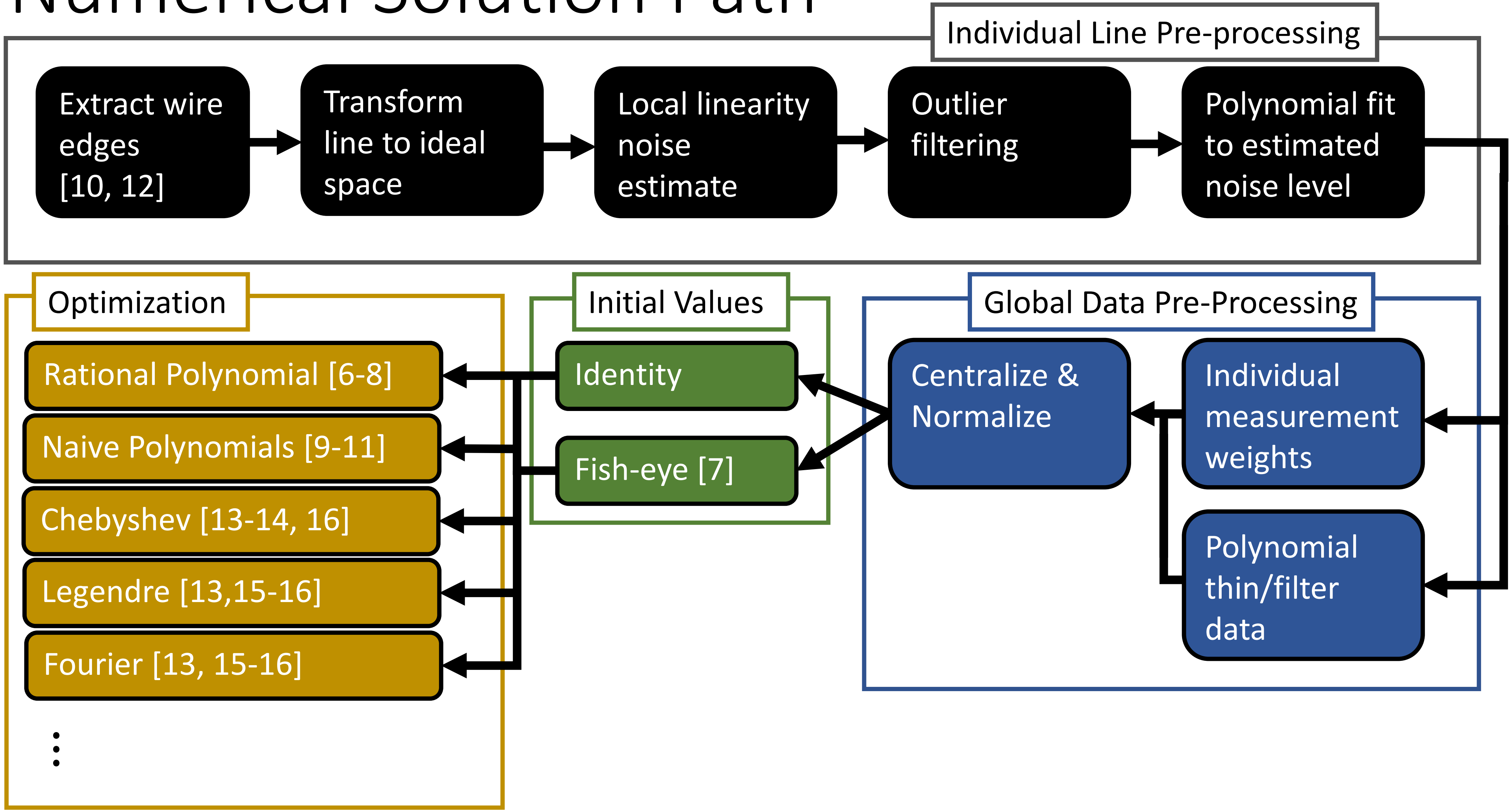

Individual Line Pre-processing

- Extract wire edges [10, 12]
- Transform line to ideal space
- Local linearity noise estimate
- Outlier filtering
- Polynomial fit to estimated noise level

Global Data Pre-Processing

- Individual measurement weights
- Polynomial thin/filter data
- Centralize & Normalize

Initial Values

- Identity
- Fish-eye [7]

Optimization

- Rational Polynomial [6-8]
- Naive Polynomials [9-11]
- Chebyshev [13-14, 16]
- Legendre [13,15-16]
- Fourier [13, 15-16]

⋮

Polymorphic Optimizer

```
interface  BasisFunction {
  //  Evaluate the basis function at (x, y)
  double operator()(double x, double y)

  // Differentiate the basis WRT x at (x, y)
  double dx(double x, double y)

  // Differentiate the basis WRT x at (x, y)
  double dy(double x, double y)
};
```

```
class  StandardPolynomialBasis implements BasisFunction {
  //  Evaluate the basis function at (x, y)
 double operator()(double x, double y)   return $x^m y^n$

  // Differentiate the basis WRT x at (x, y)
  double dx(double x, double y)            return $mx^{m-1}y^n$

  // Differentiate the basis WRT y at (x, y)
  double dy(double x, double y)            return $nx^m y^{n-1}$
};
```

Results

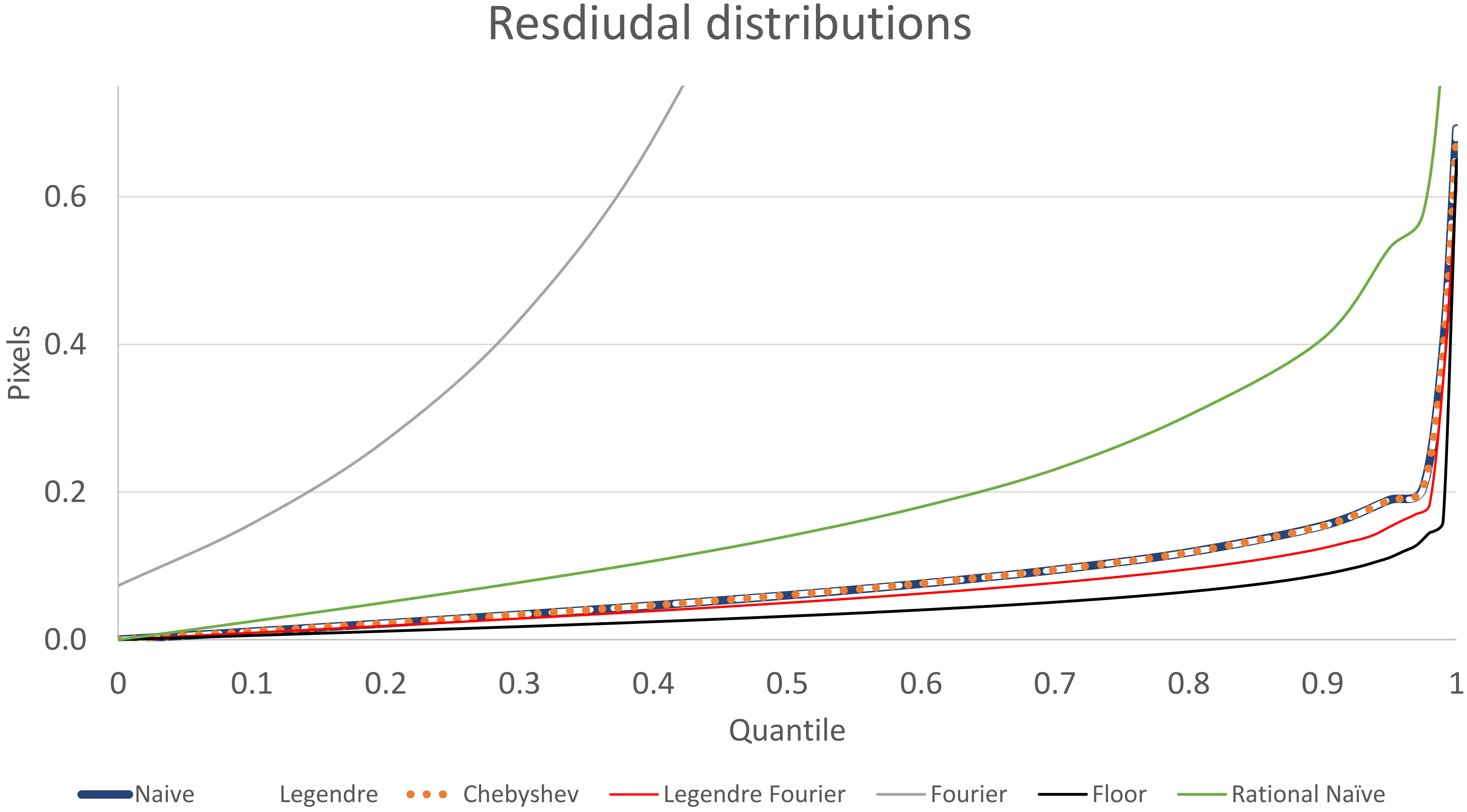
Resdiudal distributions
Pixels
0.6
0.4
0.2
0.0
0
0.1
0.2
0.3
0.4
0.5
0.6
0.7
0.8
0.9
1
Quantile
Naive
Legendre
Chebyshev
Legendre Fourier
Fourier
Floor
Rational Naïve

Results

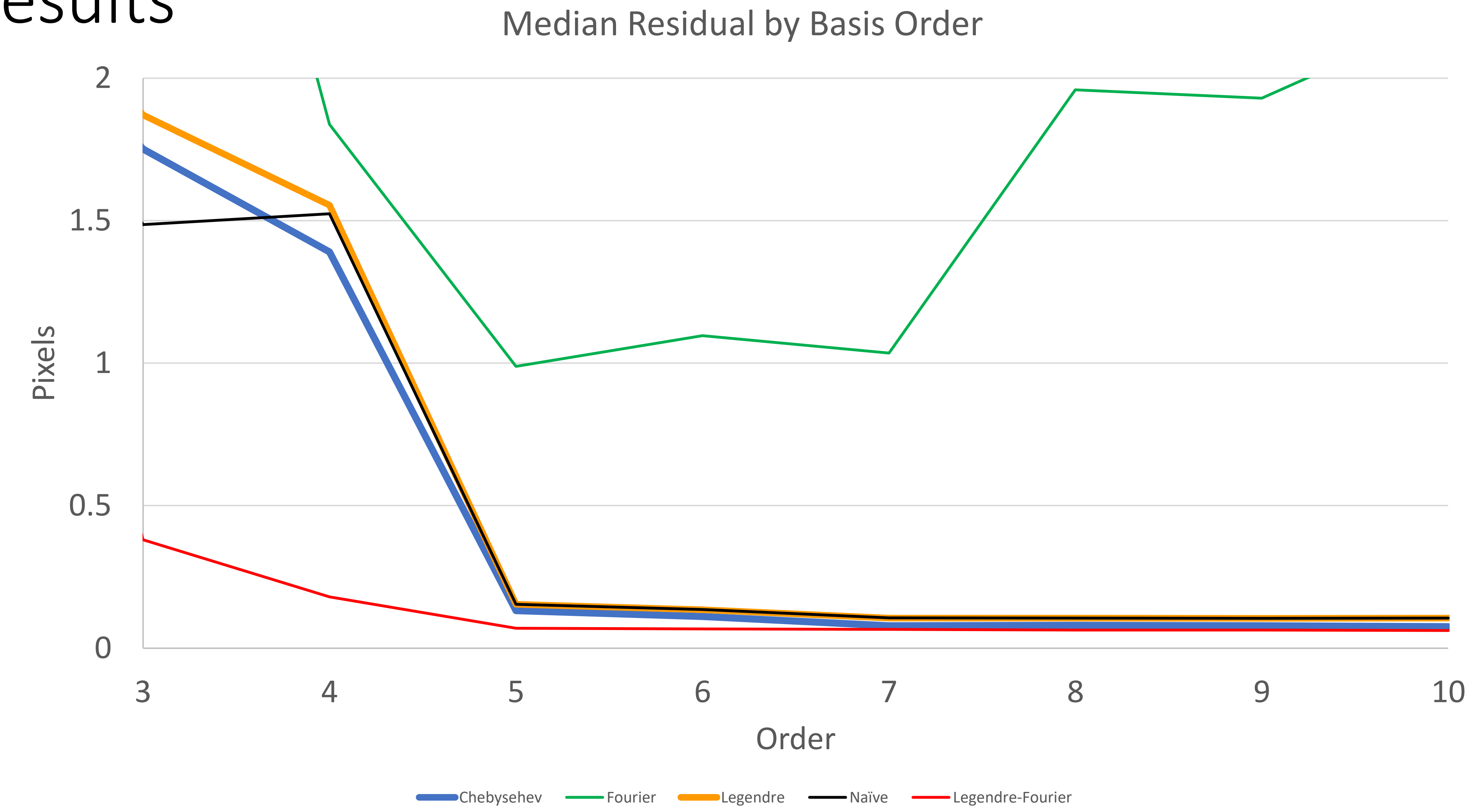
Median Residual by Basis Order
Pixels
2
1.5
1
0.5
0
3
4
5
6
7
8
9
10
Order
Chebysehev
Fourier
Legendre
Naïve
Legendre-Fourier

What happened with to Fourier basis?

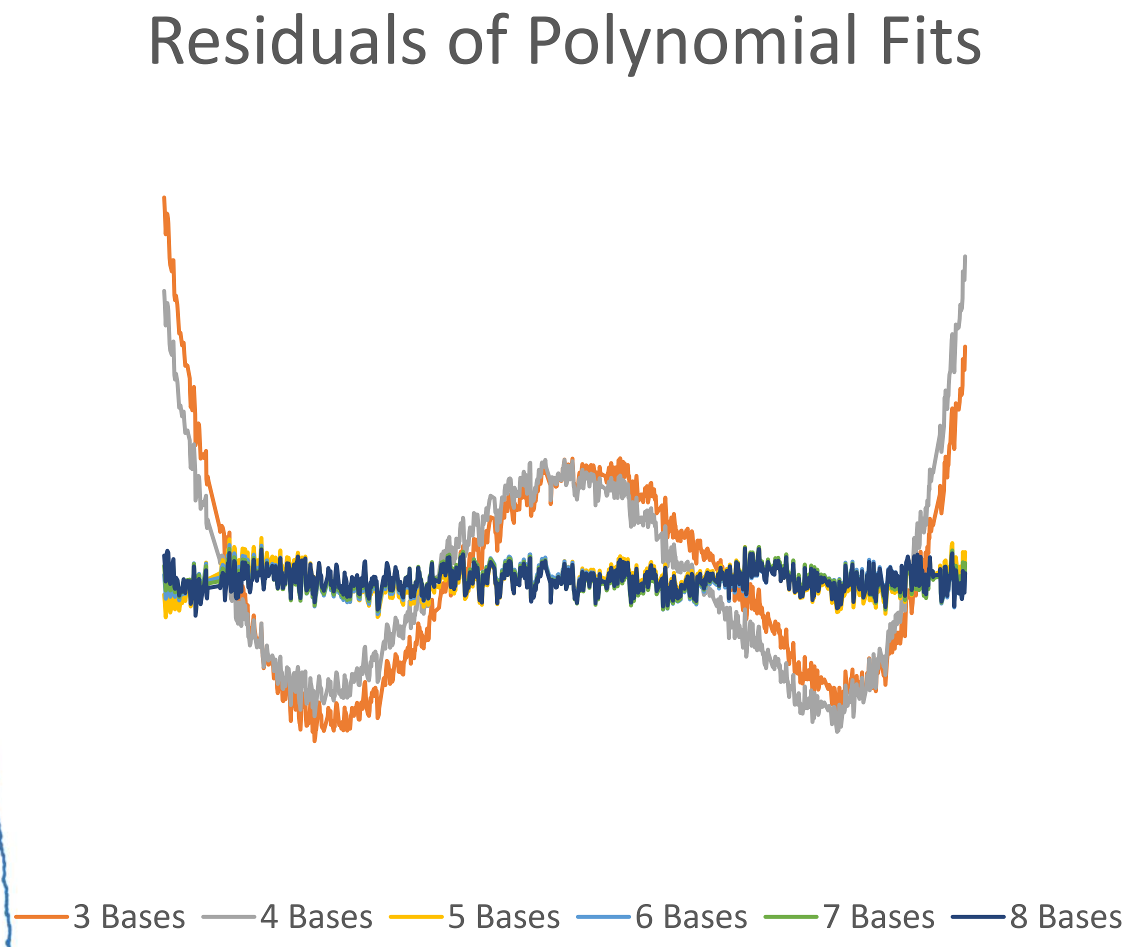

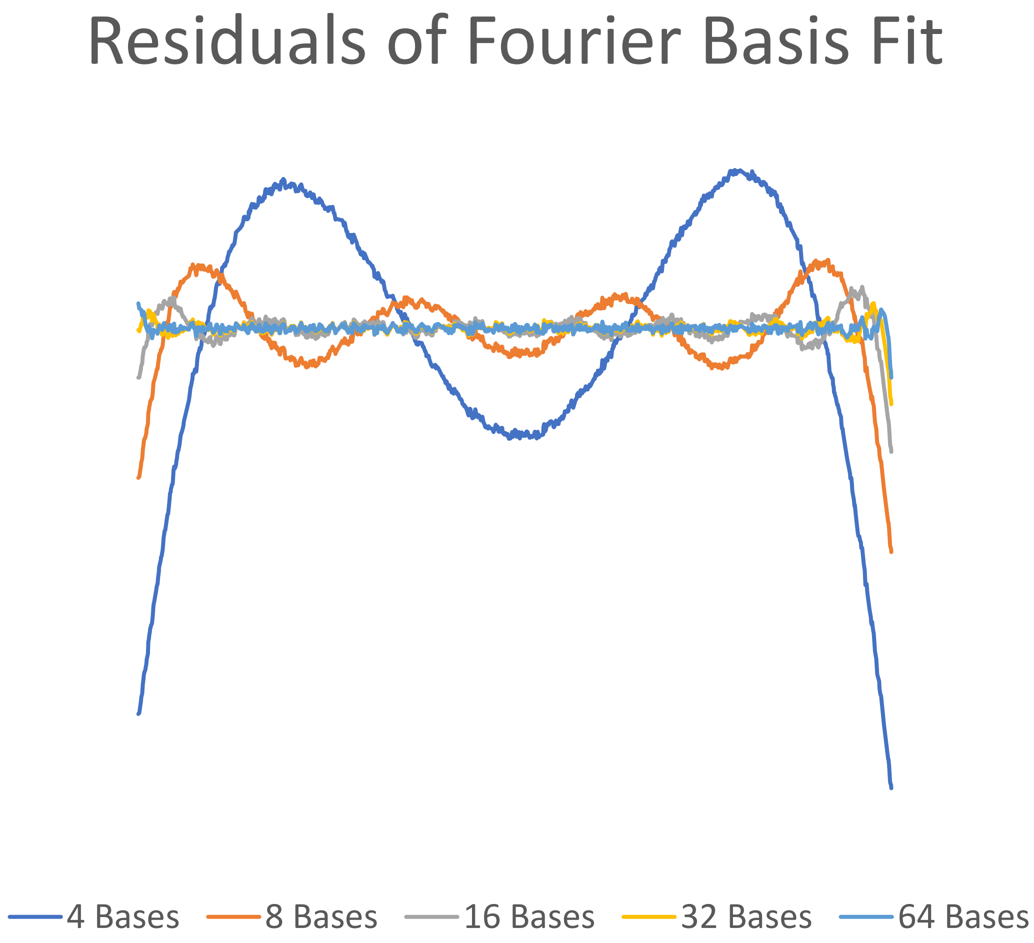

Results

Correlations

	Legendre	Chebyshev	Standard	Fourier
Percent < 0.1	95%	94%	94%	96%
99th Percentile	0.74	0.78	0.78	0.34
max	1.00	1.00	1.00	0.45

Conclusions

- Harps are a cheap and practical way to collect abundant high precision data.
- In the context of laboratory harp calibrations:
  - Orthogonal basis functions are a theoretical general approach to modeling distortion that performed well empirically.
  - The type of orthogonal basis function is largely irrelevant.
  - Polynomial bases don’t have high correlation issues they do in collinearity adjustments
  - Mixing Fourier and polynomial basis showed promise (though this is an empirical claim).

References

[1] Thompson, R. J., Danehy, P. M., Munk, M. M., Mehta, M., Manginelli, M. S., Nguyen, C., & Thomas, O. H. (2021). Stereo Camera Simulation for Lunar Surface Photogrammetry. In AIAA Scitech 2021 Forum (p. 0358).

[2] Tyrrell, O. K., Thompson, R. J., Danehy, P. M., Dupuis, C. J., Munk, M. M., Nguyen, C. P., ... & Witherow, W. K. (2022). Design of a lunar plume-surface interaction measurement system. In AIAA SCITECH 2022 Forum (p. 1693).

[3] Bouguet, J. Y. (2004). Camera calibration toolbox for matlab. http://www. vision. caltech. edu/bouguetj/calib_doc/index. html.

[4] Fetić, A., Jurić, D., & Osmanković, D. (2012, May). The procedure of a camera calibration using Camera Calibration Toolbox for MATLAB. In 2012 Proceedings of the 35th International Convention MIPRO (pp. 1752-1757). IEEE.

[5] Zhan, K., Fritsch, D., & Wagner, J. F. (2021). Stability analysis of intrinsic camera calibration using probability distributions. In IOP Conference Series: Materials Science and Engineering (Vol. 1048, No. 1, p. 012010). IOP Publishing.

[6] Tang, Z., von Gioi, R. G., Monasse, P., & Morel, J. M. (2012). High-precision camera distortion measurements with a “calibration harp”. JOSA A, 29(10), 2134-2143.

[7] Claus, D., & Fitzgibbon, A. W. (2005, September). A Plumbline Constraint for the Rational Function Lens Distortion Model. In BMVC.

[8] Claus, D., & Fitzgibbon, A. W. (2005, June). A rational function lens distortion model for general cameras. In 2005 IEEE Computer Society Conference on Computer Vision and Pattern Recognition (CVPR'05) (Vol. 1, pp. 213-219). IEEE.

[9] Rudakova, V., & Monasse, P. (2014, May). Camera matrix calibration using circular control points and separate correction of the geometric distortion field. In 2014 Canadian Conference on Computer and Robot Vision (pp. 195-202). IEEE.

[10] Devernay, F. (1995). A non-maxima suppression method for edge detection with sub-pixel accuracy (Doctoral dissertation, INRIA).

[11] Tang, Z., Von Gioi, R. G., Monasse, P., & Morel, J. M. (2017). A precision analysis of camera distortion models. IEEE Transactions on Image Processing, 26(6), 2694-2704.

[12] Chen, J., Paris, S., & Durand, F. (2007). Real-time edge-aware image processing with the bilateral grid. ACM Transactions on Graphics (TOG), 26(3), 103-es.

[13] Tang, R., Fritsch, D., Cramer, M., & Schneider, W. (2012). A flexible mathematical method for camera calibration in digital aerial photogrammetry. Photogrammetric Engineering & Remote Sensing, 78(10), 1069-1077.

[14] Ren, X., Liu, J., Li, C., Li, H., Yan, W., Wang, F., ... & Chen, W. (2019). A global adjustment method for photogrammetric processing of Chang’E-2 stereo images. IEEE Transactions on Geoscience and Remote Sensing, 57(9), 6832-6843.

[15] Huang, W., Jiang, S., & Jiang, W. (2021). Camera self-calibration with GNSS constrained bundle adjustment for weakly structured long corridor UAV images. Remote Sensing, 13(21), 4222.

[16] Tang, R. (2013). Mathematical methods for camera self-calibration in photogrammetry and computer vision.

[17] Babapour, H., Mokhtarzade, M., & Valadan Zoej, M. J. (2017). A novel post-calibration method for digital cameras using image linear features. International Journal of Remote Sensing, 38(8-10), 2698-2716.